

Article

Tracing and Evaluating Life-Cycle Carbon Emissions of Urban Multi-Energy Systems

Xiaoming Zhou ¹ , Maosheng Sang ¹, Minglei Bao ^{2,*} and Yi Ding ¹

¹ College of Electrical Engineering, Zhejiang University, Hangzhou 310063, China; xiaomingzhou@zju.edu.cn (X.Z.); 11810023@zju.edu.cn (M.S.); yiding@zju.edu.cn (Y.D.)

² College of Energy Engineering, Zhejiang University, Hangzhou 310063, China

* Correspondence: baominglei@zju.edu.cn; Tel.: +86-189-5808-7915

Abstract: With the acceleration of urbanization, urban multi-energy systems (UMESs) generate more and more carbon emissions, causing severe environmental issues. The carbon generated by UMESs includes not only emissions from the consumption of fossil fuels for electricity generation during operation phases, but also those from the transportation, extraction, and recycling of materials during construction phases. Meanwhile, as carbon emissions are delivered with the energy flow among devices in the UMES, they are distributed differently across devices. Under this background, analyzing the carbon emissions of UMESs considering different life-cycle phases (i.e., operation and construction) and carbon flow characteristics is essential for carbon reduction and environmental protection. Considering that, a novel framework for tracing and evaluating life-cycle carbon emissions of UMESs is proposed in this paper. Firstly, the carbon emission models of different devices in UMESs, including energy sources and energy hub (EH), are established considering both the construction and operation phases. On this basis, the carbon flow matrixes of EHs coupled with the energy flow model are formulated to trace the distribution of life-cycle carbon emissions in UMESs. Moreover, different evaluation indices including the device carbon distribution factor (DCDF) and consumer carbon distribution factor (CCDF) are proposed to quantify the carbon emissions of devices and consumers in UMESs. The case study results based on a typical test UMES are presented to verify the effectiveness of the proposed framework. The analysis results of the test system show that about 60% of carbon emissions are delivered to electricity loads and the construction-produced carbon emissions of energy sources and EH devices account for nearly 35% of total carbon emissions at some periods.

Keywords: urban multi-energy systems; life-cycle carbon emissions; energy hub; carbon flow



Citation: Zhou, X.; Sang, M.; Bao, M.; Ding, Y. Tracing and Evaluating Life-Cycle Carbon Emissions of Urban Multi-Energy Systems. *Energies* **2022**, *15*, 2946. <https://doi.org/10.3390/en15082946>

Academic Editor: José Matas

Received: 18 March 2022

Accepted: 13 April 2022

Published: 17 April 2022

Publisher's Note: MDPI stays neutral with regard to jurisdictional claims in published maps and institutional affiliations.



Copyright: © 2022 by the authors. Licensee MDPI, Basel, Switzerland. This article is an open access article distributed under the terms and conditions of the Creative Commons Attribution (CC BY) license (<https://creativecommons.org/licenses/by/4.0/>).

1. Introduction

A. Background

To address severe environmental issues and climate changes [1], a consensus on carbon dioxide emission (also referred to as carbon emission for brevity) reduction was achieved at the UN Climate Change Conference (COP26) by countries around the world [2]. Urban multi-energy systems (UMESs), one of the main carbon emission sources, generated around 80% of global carbon emissions with the acceleration of urbanization [3]. Under this background, evaluating the carbon emissions generated by UMESs is essential for carbon emission reduction and environmental protection.

The composition and distribution of carbon emissions in UMESs are complex, which brings some challenges to analysis. On the one hand, carbon emissions can be produced during different life-cycle phases of the UMESs, i.e., construction and operation phases [4]. For example, during the construction phase, carbon emissions may be produced by transporting, extracting, and recycling materials. According to the report of the United Nations Environment Programme, the carbon emissions during the construction phases can account

for about 30% of total life-cycle carbon emissions [5]. During the operation phase, the carbon will be emitted due to the consumption of coal or gas fuels for electricity generation [6]. On the other hand, as carbon emissions are delivered with the energy flow among devices in UMESs, they are distributed differently across devices [7]. Accurate identification of devices in UMESs with high carbon emissions is critical for carbon reduction. Therefore, it is critical to building a framework for carbon emission analysis of devices in UMESs considering both construction and operation phases as well as carbon flow characteristics.

B. Literature Review

One of the most critical issues in carbon emission analysis is to establish effective evaluation models. The carbon emission evaluating models of energy systems have been investigated extensively. Reference [8] presented a generalized model for the estimation of average displaced or avoided system emissions by intermittent renewable sources. Reference [9] presented a model based on an original indicator called trigeneration carbon emission reduction, to assess the emission reduction of carbon and other greenhouse gases from combined heat and power systems concerning the separate production. Reference [10] introduced the concept of carbon emission flow in networks. Based on the carbon emission flow theory, reference [11] formulated the carbon emission flow model in the power system sector to trace the carbon emissions associated with the flow of electricity. Reference [6] proposed an analytical model for carbon emission flow to quantify the carbon emissions associated with the energy delivery and conversion process. Reference [12] proposed a low-carbon optimal scheduling model considering demand response (DR) based carbon intensity controls. Reference [13] proposed a novel equilibrium-inspired multiagent optimization model for decentralized optimal carbon-energy combined flow of large-scale power systems. Reference [14] proposed a two-stage low-carbon operation planning model based on a bilateral trading mechanism with active demand-side management.

These evaluation models can be classified into two types: statistics-based models and trace-based models. The statistics-based models usually evaluate the carbon emissions for energy generation sides according to the emission factors of different fossil fuels [8,9]. The proposed methods can obtain the total carbon emissions of energy systems such as UMESs, but cannot determine the distribution of carbon emissions among devices. Under this circumstance, the dominant devices that cause high carbon emissions cannot be identified, which may hinder the strategy formulation of accurate carbon reduction. In order to address this problem, trace-based models are proposed to quantify the carbon emissions of each component in systems based on the energy flow models [6,10–14]. However, the previous studies mainly focus on the carbon emissions during operational phases, whereas the carbon emissions in the construction phases are seldom considered. Indeed, the carbon emissions during the construction phases can account for about 30% of total life-cycle carbon emissions [5]. Considering that, the distribution of life-cycle carbon emissions among different devices in UMESs cannot be determined precisely by the existing methods. A novel model to evaluate the life-cycle carbon emissions of UMESs needs to be developed considering the synthetical effects of system operation and construction.

In addition, the development of reasonable evaluation indices is another key to quantifying the effects of carbon emission reduction. Some research studies have put forward several carbon emission indices. Reference [15] proposed an evaluation index system for the combined cooling, heating, and power plant to qualify the relationship between economy and carbon emissions. References [16,17] proposed various evaluation indices to assess the carbon emissions of the heating pump and gas boiler in energy hubs (EHs), respectively. However, most of these evaluation indices focus on single devices, such as generator units and EH devices, and are not evaluated at the system level, which makes it difficult to effectively excavate the key devices that generate high carbon emissions in the system. In addition, these indicators usually evaluate the carbon emissions during the operation phase and neglect the construction phase, resulting in limited reference value and guiding significance. Therefore, new indices to evaluate the carbon emissions of devices and consumers in the UMES need to be proposed.

C. Contributions

Therefore, to overcome the above challenges, this paper proposes a framework for tracing and evaluating the life-cycle carbon emissions in UMESs. The major contributions of this paper are illustrated as follows:

1. A tracing method is proposed to determine the life-cycle carbon emission flow among various devices in UMESs. Specifically, the carbon emission models of different devices, including energy sources and EHs, are established considering both the construction and operation phases. On this basis, the carbon flow matrixes of the EH are developed by combining the devices' carbon emission models and the energy flow model. In this way, the distribution of life-cycle carbon emission flow in UMESs at different phases can be traced.
2. Based on the traced carbon flow, two evaluation indices are proposed to analyze the carbon emissions of devices and consumers in UMESs, including the device carbon distribution factor (DCDF) and consumer carbon distribution factor (CCDF). In specific, the DCDF index is to characterize the carbon emissions per unit of energy generated by EH devices, while the CCDF index reflects the proportion of carbon emissions delivered to consumers at different phases, such as construction and operation. Through these indicators, the key devices and consumers with high carbon emissions in the system can be identified, which can guide the formulation of carbon reduction strategies.

2. Life-Cycle Carbon Emissions of UMESs

As shown in Figure 1, the UMES mainly has two parts to satisfy the energy consumption of the consumers, i.e., the energy sources and the EH. The energy sources are the energy providers of UMESs, which mainly refer to gas flow from gas systems and electricity flow from power systems. The EH is a series of devices that converts energy to satisfy the energy consumption of consumers, which can be regarded as the connection between energy sources and consumers. At the end of UMESs, the consumers with different energy usage habits constitute electricity loads, heating loads, and cooling loads.

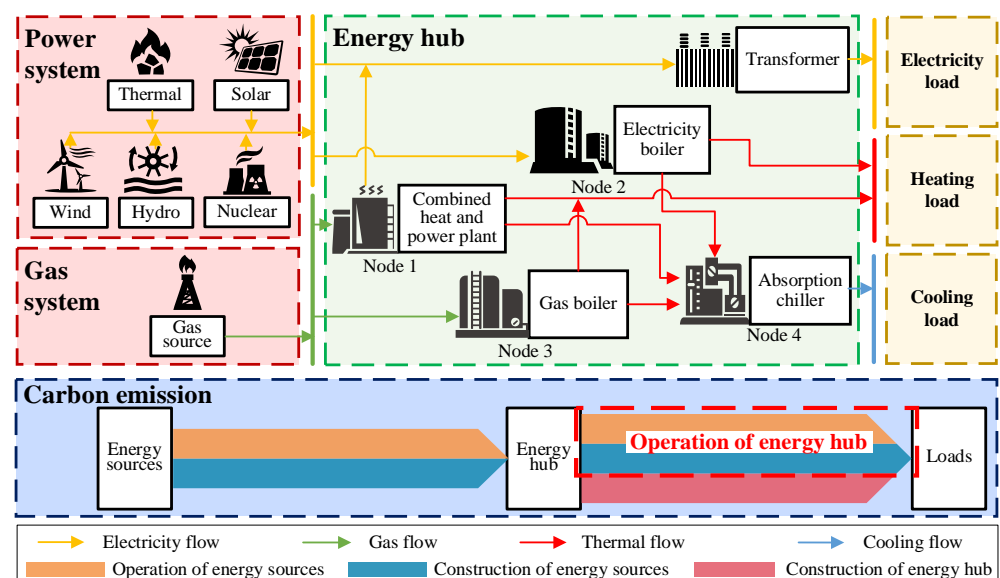


Figure 1. The framework of UMESs and their life-cycle carbon emissions.

In the life cycle, carbon emissions can be produced during the construction phase and the operation phase [4]. During the construction phase, the carbon emissions are produced by the material extraction and the device manufacture, etc. During the operation phase, the carbon emissions are produced by fossil fuel burning. In this section, the carbon

emission models of different parts, including energy sources and EHs, are established considering both the construction and operation phases.

2.1. Carbon Emissions of Energy Sources

As shown in Figure 1, the power system is combined with five types of power plants, i.e., thermal, solar, wind, hydro, and nuclear, while the gas system is combined with one type of gas production device, i.e., gas wells. Based on the structure of energy production devices in UMESs, the carbon emissions of all energy sources will be evaluated as follows.

2.1.1. Construction-Produced Carbon Emissions

Generally, the construction-produced carbon emissions are one-off during the life cycle, while the operation-produced carbon emissions exist all the time. During the operation of different devices, construction-produced carbon emissions can be distributed to the continuous energy production, which shares the same time scale as operation-produced carbon emissions. For simplicity, the carbon emissions produced during both construction and operation phases are standardized into the carbon emissions per unit of energy [10]. The standardization of construction-produced carbon emissions for different devices depends on calculating the total amount of energy generated during the devices' service lifetime. Based on the history energy generation data and load forecasting of UMESs [18], the total amount of energy generated in devices' service lifetime can be estimated as:

$$AP_{\Omega,i}^{Total} = \sum_y P_{\Omega,i,s,w,y}^{History} \times T_{\Omega,i,s,w}^{History} \times (1 + \lambda)^y, \Omega \in \{E, G, H, C\} \quad (1)$$

where, Ω represents the energy types (E represents electricity, G represents gas, H represents heating, C presents cooling). i represents the device of UMESs. $AP_{\Omega,i}^{Total}$ is the total energy generation amount in the service lifetime of device i . y represents the year. s represents the season (i.e., spring, summer, autumn, winter). w represents the day (i.e., weekday, weekend). $P_{\Omega,i,s,w,y}^{History}$ is the historical data of energy generation of device i . $T_{\Omega,i,s,w}^{History}$ is the history data of duration time of season s and day w . λ is the annual growth rate of energy generation.

Based on that, the construction-produced carbon emissions per unit of energy are modeled as the ratio of total carbon emissions and the total amount of energy generation [12].

$$c_i^{Con} = \frac{C_i^{Con}}{AP_{\Omega,i}^{Total}} \quad (2)$$

where c_i^{Con} is construction-produced carbon emissions per unit of energy generated by device i . C_i^{Con} the total construction-produced carbon emissions of device i .

Taking the power system as an example, the construction-produced carbon emissions are simultaneously related to the carbon emissions of each power plant per unit of energy, as well as the proportion of different power plants accounting for the total power output. Hence, the construction-produced carbon emissions per unit of energy $c_E^{Con}(t)$ can be estimated by the mean value of those for different power plants, which can be estimated as [18]:

$$c_E^{Con}(t) = \mathbf{c}_{Sou}^{Con} \mathbf{R}_E^{Sou}(t) \quad (3)$$

where, $c_E^{Con}(t)$ is construction-produced carbon emissions per unit of electric power supplied to the EH. $\mathbf{c}_{Sou}^{Con} = [c_{Thermal}^{Con}, c_{Solar}^{Con}, c_{Wind}^{Con}, c_{Hydro}^{Con}, c_{Nuclear}^{Con}]$ is the matrix of the construction-produced carbon emissions per unit of energy generated by different power plants, i.e., thermal, solar, wind, hydro, and nuclear. $\mathbf{R}_E^{Sou}(t) = [R_{Thermal}^{Sou}(t), R_{Solar}^{Sou}(t), R_{Wind}^{Sou}(t), R_{Hydro}^{Sou}(t), R_{Nuclear}^{Sou}(t)]^T$ is the proportion matrix of different power plants that account for the power output in power systems.

It should be noted that the proportion of power output for different power plants are fluctuating with time. Therefore, although the construction-produced carbon emissions per

unit of energy generated by different power plants are constant, the construction-produced carbon emissions per unit of energy $c_E^{Con}(t)$ can be fluctuating with time.

Since there is only one type of gas source in the gas system, the construction-produced carbon emissions per unit of gas c_G^{Con} can be seen as constant and determined by those of gas wells.

2.1.2. Operation-Produced Carbon Emissions

The carbon emissions of power systems are produced by burning fossil fuels during the operation phase. In general, solar, wind, hydro, and nuclear are clean fuels, which produce no carbon during the operation phase. The thermal power plant is the main source to produce carbon. Therefore, the operation-produced carbon emissions per unit of energy supplied to the EH. $c_E^{Ope}(t)$ is mainly determined by the thermal power, which can be calculated as [16]:

$$c_E^{Ope}(t) = c_{Thermal}^{Ope} R_{Thermal}^{Sou}(t) \quad (4)$$

where, $c_E^{Ope}(t)$ is the operation-produced carbon emissions per unit of energy. $c_{Thermal}^{Ope}$ is the operation-produced carbon emissions per unit of energy generated by thermal power plants.

In accordance with $c_E^{Con}(t)$, the operation-produced carbon emissions per unit of energy $c_E^{Ope}(t)$ are also fluctuating with time, since the proportion of power output for different power plants changes.

Likewise, the operation-produced carbon emissions per unit of gas c_G^{Ope} are constant and determined by the carbon emissions of gas wells.

2.2. Carbon Emissions of EH Devices

There are four devices in the EH, i.e., the combined heat and power plant (CHP), the electricity boiler (EB), the gas boiler (GB), and the absorption chiller (AB), as shown in Figure 1. In accordance with the power plants in the power systems, the construction-produced carbon emissions of these devices in the EH are related to the extraction and recycling processes of construction materials. Additionally, the operation-produced carbon emissions of different devices in the EH are determined by the corresponding power or gas consumption. Hence, the carbon emissions of EH during construction and operation phases are modeled as follows.

2.2.1. Construction-Produced Carbon Emissions

The total construction-produced carbon emissions of device i in EH are modeled as the carbon emissions produced by the main construction materials (aluminum, copper, polyethylene, steel, and zinc) during the construction phase. In this paper, the construction-produced carbon emissions of different construction materials produced during the extraction, manufacture, demolition, recycling, and disposal phases are set according to the data provided by reference [19] and GaBi database [16]. Additionally, the carbon emissions of different construction materials produced during the onsite phase are modeled as the transportation carbon emissions considering the weight of construction materials and the distance between the address of purchase and construction [18].

$$C_i^{EH} = \mathbf{c}_i^{Material} \mathbf{m}_i + c_i^{Transportation} \mathbf{L}_i \mathbf{m}_i \quad (5)$$

where, $\mathbf{c}_i^{Material} = [c_i^{Aluminum}, c_i^{Copper}, c_i^{Polyethylene}, c_i^{Steel}, c_i^{Zinc}]$ is the matrix of the carbon emissions per kilogram of different construction materials, i.e., aluminum, copper, polyethylene, steel, and zinc. $\mathbf{m}_i = [m_i^{Aluminum}, m_i^{Copper}, m_i^{Polyethylene}, m_i^{Steel}, m_i^{Zinc}]^T$ is the matrix of different construction materials' weight. $c_i^{Transportation}$ is the carbon emissions of device i per kilogram and kilometer. $\mathbf{L}_i = [L_i^{Aluminum}, L_i^{Copper}, L_i^{Polyethylene}, L_i^{Steel}, L_i^{Zinc}]^T$ is the matrix of the transportation distances of construction materials.

It should be noted that the data of $c_i^{Transportation}$, $c_i^{Material}$, and m_i , is selected from reference [19] and the GaBi database [16]. The L_i depends on the address of purchase and construction of different construction materials.

2.2.2. Operation-Produced Carbon Emissions

As the connection between energy sources and consumers, the EH mainly converts different types of energy to satisfy the energy consumption of consumers. Therefore, the operation-produced carbon emissions of EH are simultaneously determined by both construction-produced and operation-produced carbon emissions of energy sources.

The amount of operation-produced carbon emissions of EH is modeled as the sum of construction-produced and operation-produced carbon emissions of energy sources [11].

$$\sum_i C_i^{EH,Ope} = \left(c_E^{Con}(t) + c_E^{Ope}(t) \right) P_E^{EH}(t) \Delta t + \left(c_G^{Con} + c_G^{Ope} \right) P_G^{EH}(t) \Delta t \quad (6)$$

where, $C_i^{EH,Ope}$ is the total operation-produced carbon emissions amount of device i in EH. $P_E^{EH}(t)$ and $P_G^{EH}(t)$ are the input electricity and gas of EH, respectively. c_G^{Con} and c_G^{Ope} are the construction-produced and operation-produced carbon emissions per unit of gas and power, respectively. Δt is the step time.

It should be noted that the total operation-produced carbon emissions for EH can be determined by the amount of power and gas supplied. However, considering the energy conversion, the distribution of carbon emissions for different devices cannot be determined. Under this circumstance, the carbon emissions per unit of energy supplied to consumers cannot be determined. Hence, for calculating the amount of the embedded operation-produced carbon emissions of different devices in EH, a tracing method needs to be utilized. The specific method is proposed in Section 3 of this paper.

3. Tracing Method to Determine Life-Cycle Carbon Emission Flow of EH

Considering energy conversion features of the EH, the tracing methods are utilized for calculating the life-cycle carbon emissions of different devices. The construction-produced and operation-produced carbon emissions of energy sources and construction-produced carbon emissions of EH devices are coupled with the energy flow of EH [6]. It should be noted that the carbon emissions of energy supplied to different devices in the EH can be different. For example, as the former device, the construction-produced carbon emissions of the CHP units coupled with its outputs flow are delivered to the latter device AB. However, the construction-produced carbon emissions of the AB cannot be delivered to the CHP units due to the lack of corresponding energy flow. Therefore, the carbon emission flows through different devices are closely related to energy flows.

In this section, the energy flows of the EH are firstly modeled. On this basis, the life-cycle carbon tracing model integrated with the energy flow of the EH is proposed.

3.1. Energy Flow Model of EH

The energy flow of EH is the basis for tracing carbon emissions [6]. For calculating the energy flow in UMESs, it is important to model the devices of EH. Each device in the EH, i.e., CHP units, EB, GB, and AB, can be abstracted as a node. The topology and energy flow variables of the EH are shown in Figure 1. The inputs of the EH are electricity and natural gas, while the outputs of the EH are electricity, cooling, and heating. In normal operation, the operation objective of the EH is to minimize operating costs. Therefore, the energy flow model of the EH can be represented as (7)–(12) with the operational constraints of different devices [20]. In the proposed model, the decision variables are the energy outputs of the devices $P_{\Omega,ji}^{out}(t)$ in the EH.

$$\min f = \sum_{\Omega} \left(m_{\Omega} \times \sum_t \sum_i P_{\Omega,ji}^{out}(t) \right), j = 0 \quad (7)$$

Subject to:

$$P_{\Omega,i}^{out} = \eta_{\Omega,i} \cdot \sum_j P_{\Omega,ji}^{out}, i \in \{1, 2, 3\} \tag{8}$$

$$P_{\Omega,i}^{out} = COP_{\Omega,i} \cdot \sum_j P_{\Omega,ji}^{out}, i = 4 \tag{9}$$

$$P_{\Omega,i,-}^{out} \leq P_{\Omega,i}^{out}(t) \leq P_{\Omega,i,+}^{out}, i \in \{2, 3, 4, 5\} \tag{10}$$

$$P_{\Omega,i,-}^{ramp} \leq P_{\Omega,i}^{out}(t) - P_{\Omega,i}^{out}(t-1) \leq P_{\Omega,i,+}^{ramp} \tag{11}$$

$$\left\{ \begin{array}{l} P_{H,1}^{out}(t) \geq 0 \\ P_{E,1}^{out}(t) - P_{E,1}^A - \frac{P_{E,1}^A - P_{E,1}^B}{P_{H,1}^A - P_{H,1}^B} \times P_{H,1}^{out}(t) \leq 0 \\ P_{E,1}^{out}(t) - P_{E,1}^B - \frac{P_{E,1}^B - P_{E,1}^C}{P_{H,1}^B - P_{H,1}^C} \times (P_{H,1}^{out}(t) - P_{H,1}^B) \geq 0 \\ P_{E,1}^{out}(t) - P_{E,1}^D - \frac{P_{E,1}^C - P_{E,1}^D}{P_{H,1}^C - P_{H,1}^D} \times P_{H,1}^{out}(t) \geq 0 \end{array} \right. \tag{12}$$

where, $i, j \in \{0, 1, 2, 3, 4, 5\}$ represent the devices with the corresponding number in EH. Additionally, $i, j = 0$ represent the electricity and gas systems that supply energy. $i, j = 5$ represent the electricity/ cooling/ heating loads. $i, j = 1, 2, 3, 4$ represent the CHP units, the EB, the GB, and the AB respectively. $P_{\Omega,i}^{out}$ ($P_{\Omega,ji}^{out}(t)$) is the energy output of the device i (the device j to the device i) in energy type Ω (i.e., electricity, gas, heating, and cooling). $\eta_{\Omega,i}$ ($COP_{\Omega,i}$) is the energy conversion efficiency (coefficients of performance) of the device i in energy type Ω . m_{Ω} is the cost of unit energy Ω .

Equation (10) limits the energy generation output on devices of the EH. Equation (11) limits the energy ramp rate on devices of the EH. $P_{\Omega,1}^A, P_{\Omega,1}^B, P_{\Omega,1}^C, P_{\Omega,1}^D$ ($\Omega \in \{E, H\}$) are extreme points forming the feasible operating region of the CHP units. $P_{\Omega,i,-}^{out} / P_{\Omega,i,+}^{out}$ is the lower/ upper limits of energy capacity of the device i in energy type Ω . $P_{\Omega,i,+}^{ramp} / P_{\Omega,i,-}^{ramp}$ is the lower/ upper limits of energy ramp rate of the device i in energy type Ω . c_{Ω} is the unit price of Ω . Equation (12) represents the convex feasible operating region of the CHP units.

3.2. Life-Cycle Carbon Tracing Model Integrated with Energy Flow of the EH

Based on the results of the energy flow of EH, the life-cycle carbon emissions of EH are the sum of the construction-produced and operation-produced carbon emissions of energy sources and its own devices. Additionally, different from the construction-produced carbon emissions of the devices in EH, the construction-produced and operation-produced carbon emissions of energy sources are coupled with the same energy flow through all EH devices. Therefore, the life-cycle carbon emissions of EH devices mainly include two parts, i.e., the construction-produced and operation-produced carbon emissions of energy sources, and the construction-produced carbon emissions of the EH [21].

$$C_{\Omega,ji}^{LCA} = C_{\Omega,ji}^{Sou} + C_{\Omega,ji}^{EH} \tag{13}$$

where, $C_{\Omega,ji}^{LCA}$ represents the life-cycle carbon emission flow delivered from the device j to the device i . $C_{\Omega,ji}^{Sou}$ represents the total carbon emission flow related to energy sources delivered from the device j to the device i . $C_{\Omega,ji}^{EH}$ represents the carbon emission flow related to the construction of EH delivered from the device j to the device i .

3.2.1. Tracing Carbon Flows Related to Energy Sources

The carbon emissions of energy sources come from power plants and gas wells to consumers, including construction-produced and operation-produced ones. According to the law of carbon emission balance, the total carbon emissions of the input ports are equal to that of the output ports. Taking CHP units as an example, the carbon flows through

CHP units to its latter devices can be determined based on the corresponding energy flows, which can be represented as:

$$\begin{bmatrix} \mathbf{C}_{H,1i}^{Sou} \\ \mathbf{C}_{E,1i}^{Sou} \end{bmatrix} = \text{diag}(\underbrace{c_{H,1i'}^{Sou}, \dots}_{n_{H,1i}}, \underbrace{c_{E,1i'}^{Sou}, \dots}_{n_{E,1i}}) \begin{bmatrix} \mathbf{P}_{H,1i}^{out}(t) \\ \mathbf{P}_{E,1i}^{out}(t) \end{bmatrix} \Delta t \tag{14}$$

where, $\mathbf{P}_{H,1i}^{out}(t)$ and $\mathbf{P}_{E,1i}^{out}(t)$ are the matrix of the heating flow and electricity flow from CHP units to device i , respectively. $\mathbf{C}_{H,1i}^{Sou}$ and $\mathbf{C}_{E,1i}^{Sou}$ are the matrix of the carbon flow from CHP units to device i coupled with the heating flow and electricity flow, respectively. $n_{H,1i}$ and $n_{E,1i}$ are the amount of heating flow and electricity flow from CHP units to device i , respectively. $c_{H,1i}^{Sou}$ and $c_{E,1i}^{Sou}$ are the carbon emissions per unit of the heating flow and electricity flow from CHP units, respectively.

According to reference [11], the carbon emissions per unit of heating flow and electricity flow from CHP units are determined by the energy conversion efficiency of CHP units and the carbon emissions per unit of energy supplied to the CHP units.

$$c_{H,1i}^{Sou} = \frac{\eta_{H,1}}{\eta_{E,1}^2 + \eta_{H,1}^2} (c_G^{Con} + c_G^{Ope}) \tag{15}$$

$$c_{E,1i}^{Sou} = \frac{\eta_{E,1}}{\eta_{E,1}^2 + \eta_{H,1}^2} (c_G^{Con} + c_G^{Ope}) \tag{16}$$

In accordance with the CHP units, the carbon flows related to energy sources for each EB, GB, and AB can be calculated as:

$$\begin{bmatrix} \mathbf{C}_{H,2i}^{Sou} \\ \mathbf{C}_{H,3i}^{Sou} \\ \mathbf{C}_{C,Ai}^{Sou} \end{bmatrix} = \text{diag}(\underbrace{c_{H,2i}^{Sou}(t), \dots}_{n_{H,2i}}, \underbrace{c_{H,3i}^{Sou}, \dots}_{n_{H,3i}}, \underbrace{c_{C,Ai}^{Sou}(t), \dots}_{n_{C,Ai}}) \begin{bmatrix} \mathbf{P}_{H,2i}^{out}(t) \\ \mathbf{P}_{H,3i}^{out}(t) \\ \mathbf{P}_{C,Ai}^{out}(t) \end{bmatrix} \Delta t \tag{17}$$

where, $\mathbf{P}_{H,2i}^{out}(t)$, $\mathbf{P}_{H,3i}^{out}(t)$, and $\mathbf{P}_{C,Ai}^{out}(t)$ are the matrix of the heating flow from EB, the heating flow from GB, and the cooling flow from AB to device i , respectively. $\mathbf{C}_{H,2i}^{Sou}$, $\mathbf{C}_{H,3i}^{Sou}$, and $\mathbf{C}_{C,Ai}^{Sou}$ are the matrix of the carbon flow from EB, GB, and AB to device i coupled with energy flow, respectively. $n_{H,2i}$, $n_{H,3i}$, and $n_{C,Ai}$ are the amount of energy flow from EB, GB, and AB to device i , respectively. $c_{H,2i}^{Sou}(t)$, $c_{H,3i}^{Sou}$, and $c_{C,Ai}^{Sou}(t)$ are the carbon emissions per unit of the heating flow and electricity flow from EB, GB, and AB, respectively.

The carbon emissions per unit of heating flow and electricity flow from EB, GB, and AB are determined by the energy conversion efficiency of these devices, and the carbon emissions per unit of energy supplied to these devices [11].

$$c_{H,2i}^{Sou}(t) = \frac{(c_E^{Con}(t) + c_E^{Ope}(t))}{\eta_{H,2}} \tag{18}$$

$$c_{H,3i}^{Sou} = \frac{(c_G^{Con} + c_G^{Ope})}{\eta_{H,3}} \tag{19}$$

$$c_{C,Ai}^{Sou}(t) = \frac{\sum_j (c_{H,j4}^{Sou}(t) \times P_{H,j4}^{out}(t)) / \sum_j P_{H,j4}^{out}(t)}{COP_{CA}} \tag{20}$$

3.2.2. Tracing Construction-Produced Carbon Related to Energy Hub

In EH, the CHP units, EB, and GB correspond to former devices since they are supplied by electricity or gas energy systems directly. Therefore, the construction-produced carbon flow of these devices to the latter devices can be determined based on the corresponding energy flows, which can be calculated as:

$$\mathbf{C}_{\Omega,ji}^{EH} = \text{diag}(\underbrace{c_1^{EH}, \dots, c_2^{EH}}_{n_{H,1i}+n_{E,1i}}, \underbrace{c_3^{EH}, \dots, c_4^{EH}}_{n_{H,2i}}, \dots) \mathbf{P}_{\Omega,ji}^{out}(t) \Delta t \quad (21)$$

where, $\mathbf{P}_{\Omega,ji}^{out}(t) = [P_{\Omega,ji}^{out}(t)]$ is the matrix of energy flows from device j to device i . $\mathbf{C}_{\Omega,ji}^{EH}$ is the matrix of construction-produced carbon flow of different devices coupled with energy flow from CHP units, EB, and GB to device i .

Moreover, the AB corresponds to the latter devices in EH because it is supplied by energy flows from the CHP units, EB, and GB. Therefore, the construction-produced carbon flow of AB is modeled as the sum of construction-produced carbon emissions of itself and delivered from the former devices.

$$\mathbf{C}_{\Omega,Ai}^{EH} = \text{diag}(\underbrace{c_4^{EH}, \dots}_{n_{C,Ai}}) \mathbf{P}_{C,Ai}^{out}(t) \Delta t + \text{diag}(\underbrace{c_{4,in}^{EH}(t), \dots}_{n_{C,Ai}}) \mathbf{P}_{C,Ai}^{out}(t) \Delta t \quad (22)$$

$$c_{4,in}^{EH}(t) = \frac{\sum_j (c_j^{EH}(t) \times P_{H,j4}^{EH}(t)) / \sum_j P_{H,j4}^{EH}(t)}{COP_{CA}} \quad (23)$$

where, $\mathbf{C}_{\Omega,Ai}^{EH}$ is the matrix of construction-produced carbon flow from AB to device i coupled with the cooling flow. $c_{4,in}^{EH}(t)$ is the construction-produced carbon emissions per unit of energy supplied from the former devices.

Considering the combination between life-cycle carbon flows related to energy sources in Equation (13) and EH in Equation (23), the life-cycle carbon flows delivered from the device j to the device i in the EH can be calculated as:

$$\begin{aligned} \mathbf{C}_{\Omega,ji}^{LCA} &= \mathbf{C}_{\Omega,ji}^{Sou} + \mathbf{C}_{\Omega,ji}^{EH} \\ &= \mathbf{c}_{ji}^{LCA}(t) \mathbf{P}_{\Omega,ji}^{out}(t) \Delta t \end{aligned} \quad (24)$$

where, $\mathbf{C}_{\Omega,ji}^{LCA}$ is the matrix of the life-cycle carbon emission flow delivered from the device j to the device i . $\mathbf{C}_{\Omega,ji}^{Sou}$ is the matrix of the carbon flows (related to energy sources) delivered from the device j to the device i . $\mathbf{C}_{\Omega,ji}^{EH}$ is the matrix of the carbon flows (related to EH construction) delivered from the device j to the device i . $\mathbf{c}_{ji}^{LCA}(t)$ is the matrix of the carbon emissions per unit of energy delivered from the device j to the device i .

4. Evaluation of Life-Cycle Carbon Emissions of UMESs

4.1. Evaluation Indices

To precisely reduce carbon emissions, a set of indices for accurate carbon assessment of UMESs is required. Most traditional evaluation indices focus on single devices, such as generator units [15] and EH devices [16], and are not evaluated at the system level. However, it is difficult to effectively excavate the key devices that generate high carbon emissions in the system by evaluating single devices. The reasonable evaluation of devices and consumers with higher carbon emissions is critical to achieving precise carbon reductions of UMESs. In order to analyze the carbon emissions among various devices and consumers in UMESs, the device carbon distribution factor (DCDF) and consumer carbon distribution factor (CCDF) are proposed in this paper. On this basis, the evaluation procedures for life-cycle carbon emissions of UMESs are illustrated in this section.

(1) Device Carbon Distribution Factor

Since the UMESs devices may have multiple energy flows at the same time, and their energy types and amounts are different, the life-cycle carbon emissions per unit of energy distributed in each device cannot be simply obtained by averaging them corresponding to each energy flow. Therefore, this paper proposed the DCDF index to characterize the life-cycle carbon emissions per unit of energy. The total life-cycle carbon emissions distributed in device j can be calculated by the proposed life-cycle carbon tracing method. The total

amount of energy generated by device j can be calculated by the energy flow model. As shown in Figure 2a, the DCDF index can be calculated as the ratio of the total life-cycle carbon emissions distributed in each device to the total amount of energy generated by the corresponding device.

$$DCDF_j^{LCA}(t) = \frac{C_j^{Total}(t)}{W_j^{Total}(t)} = \frac{\sum_{\Omega} \sum_i C_{\Omega,ji}^{LCA}(t)}{\sum_{\Omega} \sum_i P_{\Omega,ji}^{out}(t) \Delta t} \quad (25)$$

where, the $DCDF_j^{LCA}(t)$ is the DCDF index of device j . $C_j^{Total}(t)$ is the total life-cycle carbon emissions distributed in device j . $W_j^{Total}(t)$ is the total amount of energy generated by device j .

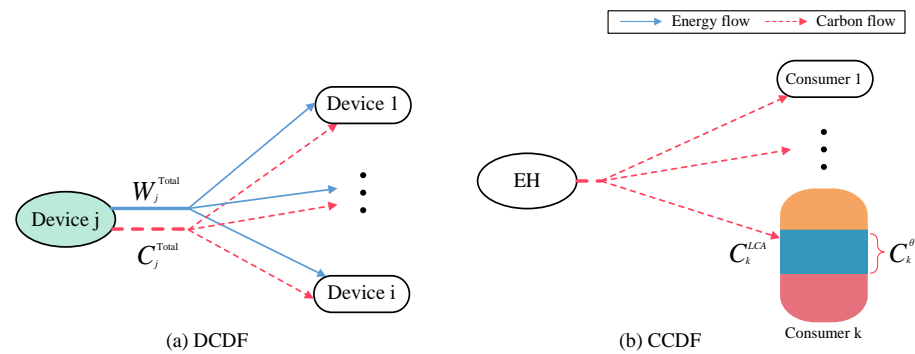


Figure 2. DCDF index and CCDF index.

It should be noted that some devices in the EH will have no carbon distribution since their energy generation is zero during certain periods. In these special cases, the DCDF value is set as zero.

(2) Consumer carbon distribution factor

Since different consumers have different energy usage habits, the carbon emission composition of different consumers will be different. If consumers use more energy supplied by the EH, they will contain more construction-produced carbon emissions of EH than consumers who use more energy supplied by the power system. Therefore, this paper proposed the CCDF index to reflect the proportion of carbon emissions delivered to consumers at different phases, such as construction and operation. The carbon emissions produced during different phases can be calculated as the product of the consumers' energy consumption and corresponding carbon emissions per unit of energy. It should be noted that the life-cycle carbon emissions of consumers need to be calculated by the total life-cycle carbon emissions and the total energy consumption of energy loads. As shown in Figure 2b, the CCDF index can be calculated as the ratio of the carbon produced during different phases to the life-cycle carbon emissions of consumers.

$$CCDF_k^\theta(t) = \frac{C_k^\theta(t)}{C_k^{LCA}(t)} = \frac{\sum_{\Omega} \sum_j (P_{\Omega,jk}(t) \times c_{\Omega,j5}^\theta(t))}{\sum_{\Omega} \left(\sum_j P_{\Omega,jk}(t) \times \frac{\sum_j C_{\Omega,j5}^{LCA}(t)}{\sum_j P_{\Omega,j5}^{out}(t)} \right)} \Delta t \quad (26)$$

where, θ presents the carbon type (i.e., energy sources construction, energy sources operation, energy hub construction). k presents the consumer. $CCDF_k^\theta(t)$ is the CCDF index during phase θ of consumer k . $C_k^\theta(t)$ is the carbon emissions produced during phase θ and delivered to consumer k . $C_k^{LCA}(t)$ is the life-cycle carbon emissions delivered to consumer k . $P_{\Omega,jk}(t)$ is the energy consumption of consumer k . $c_{\Omega,j5}^\theta(t)$ is the carbon emissions per unit

of energy generated during phase θ . $C_{\Omega,j5}^{LCA}(t)$ is the life-cycle carbon emissions delivered to energy loads. $P_{\Omega,j5}^{out}(t)$ is the number of energy loads.

In this paper, all types of energy loads are nonzero during any period. If some consumers do not have any energy consumption during certain periods, the CCDF value will be set as zero.

4.2. Evaluation Processes

As shown in Figure 3, For evaluating the life-cycle carbon emissions of UMESs, there are eight steps in the evaluation process:

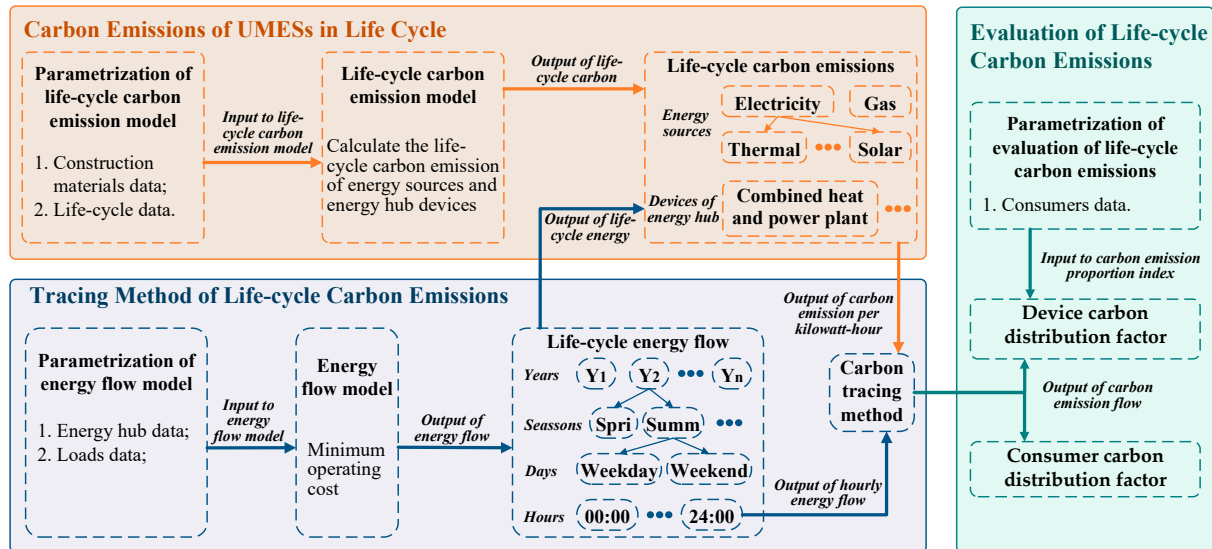


Figure 3. Flowchart of carbon emission evaluation of UMESs.

Step 1. Input life-cycle data of different power plants and gas wells. The data can include annual construction-produced and operation-produced carbon emissions per unit of energy generated by different energy sources, e.g., the annual construction-produced and operation-produced carbon emissions per unit of energy generated by thermal power plants.

Step 2. Input life-cycle data of different devices of EH, e.g., the types of construction materials and their weight, the life-cycle carbon emissions of construction materials per kilogram, the transportation distance between purchase and construction, and the carbon emissions of transportation per kilogram per kilometer.

Step 3. Utilize Equation (5) to calculate the amount of life-cycle carbon emissions of different EH devices during the construction phase considering different construction materials and their transportation.

Step 4. Input EH data, i.e., the serving time of devices, the history of energy flow on weekdays and weekends in four seasons, the output limit of devices, the ramp rate limit of devices, and the energy conversion efficiency (coefficients of performance) of devices.

Step 5. Based on the results of Step 3 and Step 4, utilize Equation (2) to calculate the construction-produced carbon emissions per unit of energy generated by EH devices, considering the multi-energy loads' fluctuation among weekdays and weekends in four seasons.

Step 6. Utilize Equations (7)–(12) to calculate the energy flow and the outputs of devices in EH for the economy. In this step, energy conversion and energy sources costs are considered.

Step 7. Utilize Equations (13)–(24) to calculate the carbon flow generated by different devices in UMESs. Additionally, each energy flow in UMESs consists of the operation-produced and construction-produced carbon emissions of energy sources and the construction-produced carbon emissions of EH devices, which are calculated respectively.

Step 8. Utilize Equation (25) to calculate the DCDF index and utilize Equation (26) to calculate the CCDF index.

5. Case Studies

5.1. Test System and Parameters

The test system is a typical UMES [22], of which the structure is shown in Figure 1. The construction-produced and operation-produced carbon emission parameters of energy sources are presented in Table 1 [23,24]. The construction materials data of EH devices including CHP units [21], EB [17], GB [17], and AB [17] are presented in Table 2. Additionally, the transportation-produced carbon emission parameters of all EH devices are set as 271.6 g/t*km, and the transportation distances of construction materials are set as 900 km. The operation parameters of EH devices [25], including the capacity and ramp rate, are presented in Tables 3 and 4. The electricity, heating, and cooling loads in four seasons are presented in Figure A1 of Appendix A [22].

Table 1. Carbon emission parameters of energy sources in the test system (g/kWh).

Phases	Thermal	Solar	Wind	Hydro	Nuclear	Gas
Construction	215.6	89.9	18	12.75	11.9	19
Operation	785	0	0	0	0	283

Table 2. Construction materials data of EH devices in the test system.

	CHP Units (kg)	EB (kg)	GB (kg)	AB (kg)	Unit Carbon Dioxide Emissions (kg/kg) [19]
Aluminum	0.5	0	780	5040	11.6
Copper	672.1	7700	320	5760	2.7
Zinc	0.808	0	0	240	5.19
Steel	26790.9	33250	12500	44400	1.46
Polyethylene	267.8	350	95	480	1.462

Table 3. Capacities of EH devices in the test system (kW).

$P_{H,1}^A$ 0	$P_{E,1}^A$ 2500	$P_{H,1}^B$ 1100	$P_{E,1}^B$ 2100	$P_{H,1}^C$ 900	$P_{E,1}^C$ 500
$P_{H,1}^D$ 0	$P_{E,1}^D$ 1000	$P_{H,2,-}^{out}$ 200	$P_{H,2,+}^{out}$ 2500	$P_{H,3,-}^{out}$ 200	$P_{H,3,+}^{out}$ 2500
$P_{C,4,-}^{out}$ 200	$P_{C,4,+}^{out}$ 4500	$P_{C,5,-}^{out}$ 0	$P_{C,5,+}^{out}$ 3000	$P_{C,v,-}^{EH}$ 0	$P_{C,v,+}^{EH}$ 2

Table 4. Ramp rate of EH devices in the test system (kW/s).

$P_{H,1,-}^{ramp}$ −739.2	$P_{H,1,+}^{ramp}$ 739.2	$P_{E,1,-}^{ramp}$ −554.4	$P_{E,1,+}^{ramp}$ 554.4	$P_{H,2,-}^{ramp}$ −2000	$P_{H,2,+}^{ramp}$ 2000
$P_{H,3,-}^{ramp}$ −1250	$P_{H,3,+}^{ramp}$ 1250	$P_{C,4,-}^{ramp}$ −18,000	$P_{C,4,+}^{ramp}$ 18,000	$P_{C,5,-}^{ramp}$ −6000	$P_{C,5,+}^{ramp}$ 6000

5.2. Analysis Results

(1) Carbon emissions of energy sources and EH devices

According to Equations (3) and (4), the carbon emissions per unit of energy generated by energy sources in the four seasons are calculated and illustrated in Figure 4, wherein the dotted line, dashed line and solid line denote the construction-produced, operation-produced, and life-cycle carbon emissions, respectively. In addition, the generation proportion of different energy sources is also displayed in Figure 4. It can be seen that the operation-produced carbon emissions fluctuate with the generation trend of thermal plants because they are mainly produced by thermal power plants. Different from the operation-produced carbon emissions, the construction-produced carbon emissions of different energy resources have no significant difference over the course of the year so the

dotted lines are nearly flat in four seasons. Note that as shown in Figure 4b, the output of solar power generation increases around 12:00 in summer, so the operation-produced carbon emissions stay at the lowest level of the year and the construction-produced carbon emissions account for nearly 35% of total carbon emissions.

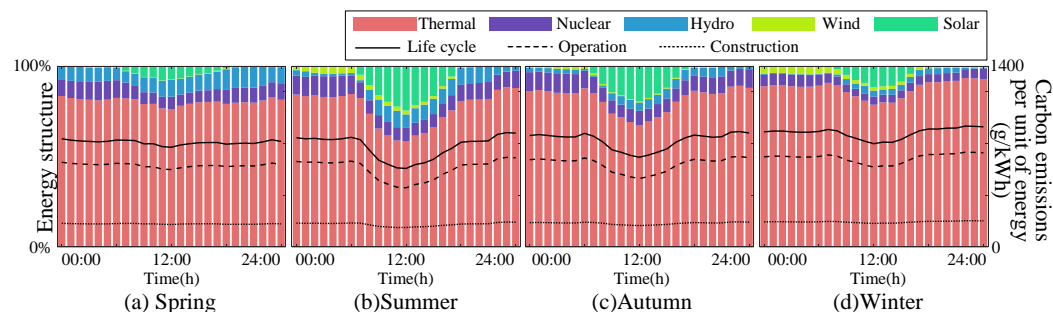


Figure 4. Carbon emissions results and generation proportion of different energy sources in four seasons.

The carbon emissions results of various EH devices are calculated and listed in Table 5. It can be seen that the AB has the most total construction-produced carbon emissions of 12325 t, while it does not produce the largest construction-produced carbon emissions per unit of energy generated. The EB has the most construction-produced carbon emissions per unit of energy generated at 245.7 g/kWh. The GB has the least total construction-produced carbon emissions amount of 2525 t, and the most total energy generation of 135 GW. Therefore, among EH devices, the GB produces the lowest construction-produced carbon emissions per unit of energy generated, at 18.7 g/kWh.

Table 5. Carbon emissions results of EH devices.

	CHP Units	EB	GB	AB
Total construction-produced carbon emissions amount (t)	3870	6388	2525	12325
Total energy generation (GW)	37	26	135	58
Construction-produced carbon emissions per unit of energy generated (g/kWh)	104.6	245.7	18.7	212.5

(2) Carbon emission flow of the UMES

The carbon emission flow of the test system on a summer weekday is shown in Figure 5, in which the amount of carbon emission flow is represented by the width of the color band. In addition, the inputs and outputs of the EH in the test system on summer weekdays are presented in Figure A2 of Appendix A, and the results of the proposed method are compared with the operation-produced carbon emissions tracing method, as shown in Table 6. Figure 5 shows that the operation-produced carbon flow comes from two sources, i.e., thermal plants and gas sources, while the construction-produced carbon flow comes from more sources, including solar plants, wind plants, hydro plants, and nuclear plants. Note that in the test system, the capacity of thermal plants is much higher than that of other power plants, so the amount of the construction-produced carbon flow of thermal plants is the highest in the system. Moreover, although the gas consumption and electricity consumption are close throughout the day as shown in Figure A2a, the operation-produced carbon emissions of the power system are higher than the gas system.

In this test system, the energy flow of electricity loads is mainly delivered from the power system directly, while that of cooling loads and heating loads are mainly delivered from the gas system through EH devices such as the GB and CHP units, as shown in Figure 5. Therefore, the carbon emission flow of EH devices is mainly delivered to cooling loads and heating loads, while that of energy sources is mainly delivered to electricity loads.

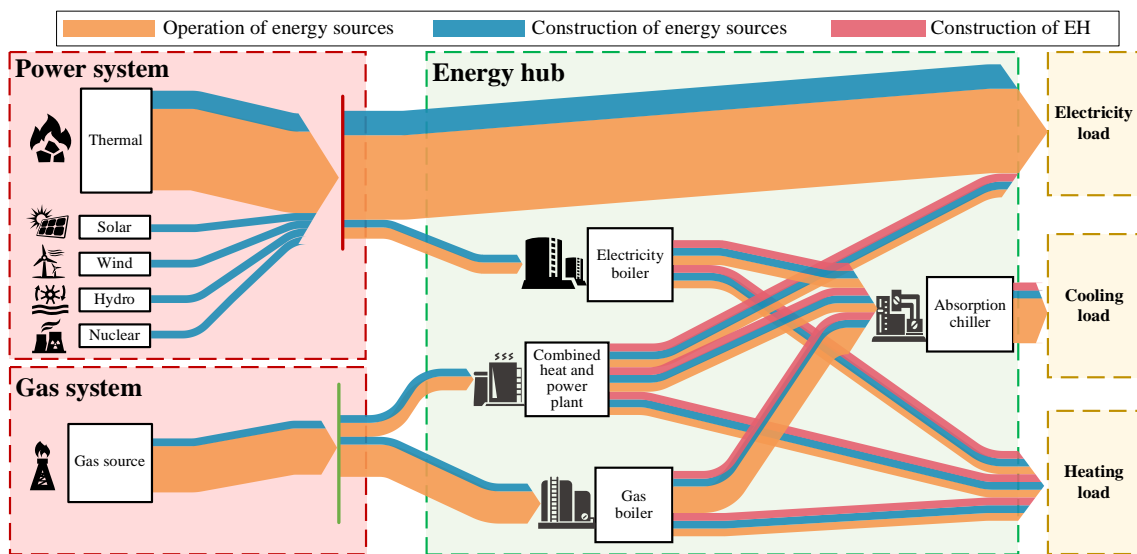


Figure 5. The carbon emission flow of the UMES on a summer weekday.

Table 6. Carbon flow of EH devices throughout the day of a summer weekday (kg).

Former Device	Operation-Produced Carbon Emissions of Energy Sources				
	Thermal	Gas Source	Power System	Power System	Gas System
Latter device Carbon emission	Power system 8500.73	Gas system 4488.18	Electricity boiler 1094.07	Electricity load 7406.65	Combined heat and power plant 1354.78
Former device	Gas system	Combined heat and power plant	Combined heat and power plant	Combined heat and power plant	Electricity boiler
Latter device Carbon emission	Gas boiler 3133.39	Absorption chiller 867.06	Heating load 0	Electricity load 487.72	Absorption chiller 907.41
Former device	Operation-produced carbon emissions of energy sources				Construction-produced carbon emissions of energy sources
Latter device Carbon emission	Electricity boiler Heating load 186.65	Gas boiler Absorption chiller 2578.32	Gas boiler Heating load 555.07	Absorption chiller Cooling load 4352.8	Thermal Power system 1898.24
Former device	Construction-produced carbon emissions of energy sources				
Latter device Carbon emission	Nuclear Power system 221.8	Hydro Power system 133.14	Wind Power system 49.13	Solar Power system 145.6	Gas source Gas system 301.32
Former device	Construction-produced carbon emissions of energy sources				
Latter device Carbon emission	Power system Electricity boiler 303.63	Power system Electricity load 2144.3	Gas system Combined heat and power plant 90.95	Gas system Gas boiler 210.36	Combined heat and power plant Absorption chiller 58.21
Former device	Construction-produced carbon emissions of energy sources				
Latter device Carbon emission	Combined heat and power plant Heating load 0	Combined heat and power plant Electricity load 32.74	Electricity boiler Absorption chiller 251.84	Electricity boiler Heating load 51.79	Gas boiler Absorption chiller 173.1
Former device	Construction-produced carbon emissions of energy sources		Construction-produced carbon emissions of EH devices		
Latter device Carbon emission	Gas boiler Heating load 37.26	Absorption chiller Cooling load 483.15	Combined heat and power plant Absorption chiller 200.36	Combined heat and power plant Heating load 0	Combined heat and power plant Electricity load 150.27
Former device	Construction-produced carbon emissions of EH devices				
Latter device Carbon emission	Electricity boiler Absorption chiller 283.67	Electricity boiler Heating load 58.23	Gas boiler Absorption chiller 161.8	Gas boiler Heating load 34.83	Absorption chiller Cooling load 1619.41

Furthermore, the carbon emissions of the UMES during 24 h of the day are shown in Figure 6. It can be seen that the carbon emission results vary in different periods due to changing load demands. The carbon emissions are classified by life cycle phases and energy load types as shown in Figure 6a,b, respectively. Figure 6a shows that the operation-produced carbon emissions generated by energy sources account for the largest proportion, while Figure 6b indicates that the most carbon emissions are delivered to electricity loads.

Additionally, the construction-produced carbon emissions of EH devices during 8:00–18:00 are larger than in other periods due to the significant increase in cooling loads, as shown in Figure A2b.

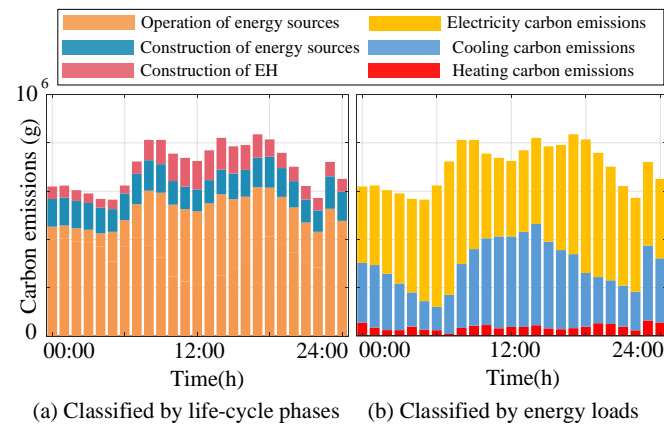


Figure 6. The carbon emissions of the UMES in 24 h of a summer weekday.

(3) Evaluation indices

According to Equation (25), the DCDF indices of various EH devices are calculated and illustrated in Figure 7. It can be seen that the DCDF indices of CHP units and GB stay at a low level, indicating the carbon emissions per unit of energy distributed in them are small. This is because the CHP units and GB are mainly powered by gas fuel. Moreover, the DCDF index of AB also stays at a low level during 7:00–22:00, because the heating to AB is provided by GB during this period and EB during other periods.

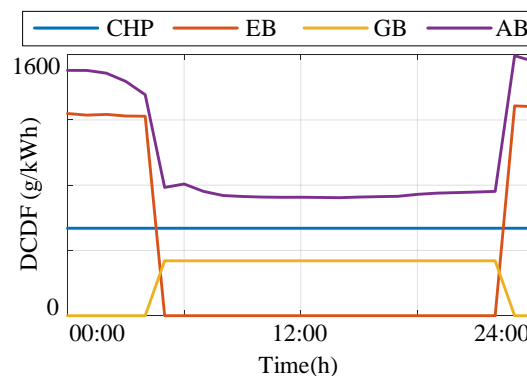


Figure 7. The DCDF values of various EH devices.

According to Equation (26), the CCDF indices of two different consumers (i.e., Consumer A and Consumer B) at two periods are calculated and shown in Figure 8. It is assumed that Consumer A only has electricity-driven thermostatically controlled loads for cooling, while Consumer B has multi-energy-driven thermostatically controlled loads. The ratio of multi-energy consumption (i.e., electricity: heating: cooling) is 9:0:1 for Consumer A and 5:1:4 for Consumer B. In this paper, the circumstances of Consumer A and B at 00:00 are denoted as A1 and B1, respectively. Likewise, the circumstances of Consumer A and B at 12:00 are denoted as A2 and B2, respectively.

As shown in Figure 8, the EH construction-produced CCDF value of Consumer B is larger than that of Consumer A. That is because Consumer B has more cooling loads than Consumer A, which delivered more construction-produced carbon emissions of EH devices. Meanwhile, the energy structure is different during different periods. As shown in Figure 8, the energy source operation-produced CCDF value at A1 is larger than that at A2. That is because the energy generation of renewable energy resources (e.g., solar power

plants) is small while that of thermal plants is large at 00:00 than those at 12:00, as shown in Figure 8b.

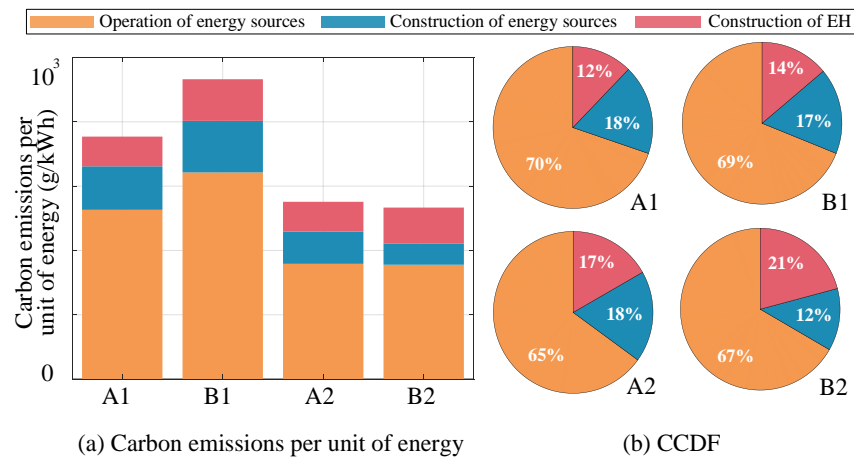


Figure 8. The CCDF index of two consumers with different energy usage habits at two periods.

To verify the applicability and generality of the framework proposed in this paper, a more complex UMES is used for simulation. Compared with the original test system, the number of consumers with complicated energy usage habits has increased by five times. The carbon emission flow of this more challenging case can be successfully traced by the proposed method, and the calculation results are appended in Figure 9. The results show that the carbon emissions of the gas system in this complex network are significantly higher than the power system because the EH is mainly responsible for the user’s energy demand in the complex system. Compared with the original system, the construction-produced carbon emissions of EH devices per unit of energy in the complex system are reduced. This is due to the higher frequency of use of EH devices, as introduced in Section 2.2. Moreover, the total carbon emissions of users in this complex system drop. This is because the dependence of this complex system on natural gas has greatly increased compared to the original network. The results show that the framework proposed in this paper is universal for complex systems.

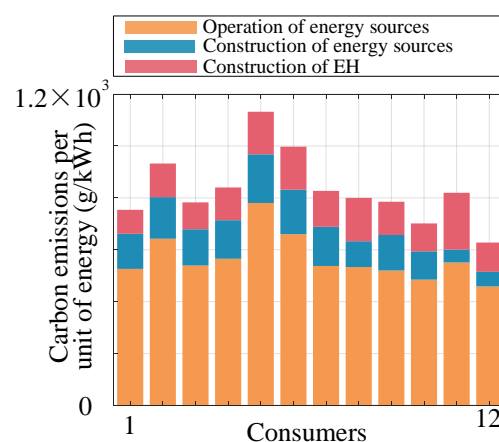


Figure 9. Carbon emissions per unit of energy.

5.3. Discussion

Based on the proposed framework, the distribution of life-cycle carbon emission flow in UMESs at both the construction and operation phases can be traced. Numerical results indicate that about 60% of carbon emissions are delivered to electricity loads and the construction-produced carbon emissions of energy sources and EH devices account for nearly 35% of total carbon emissions at some periods. Accurate identification of devices

in UMESs with high carbon emissions can guide the formulation of carbon reduction strategies. Additionally, the DCDF index can help system operators identify devices with high carbon emissions and the corresponding time periods, based on which effective operation strategies can be developed for carbon emission reduction. The CCDF index can help system operators find out critical consumers with high carbon emissions in the UMES to implement precise carbon emission reduction controls.

6. Conclusions

This paper proposes a framework for tracing and evaluating the life-cycle carbon emissions of UMESs, considering both the construction and operation phases. A tracing method is proposed to determine the life-cycle carbon emission flow among various devices in UMESs. Specifically, the carbon emission models of different devices, including energy sources and EHs, are established considering both the construction and operation phases. On this basis, the carbon flow matrixes of the EH are developed by combining the devices' carbon emission models and the EH energy flow model. Based on the traced carbon flow, evaluation indices are proposed to analyze the carbon emissions of each device and consumer in the UMES, including the DCDF index and CCDF index. The case study based on a realistic UMES is conducted to verify the effectiveness of the proposed framework. Numerical results indicate that thermal plants are the most carbon emissions devices in UMESs, and most carbon emissions are delivered to electricity loads. The construction-produced carbon emissions of energy sources and EH devices account for nearly 35% of total carbon emissions at some periods.

The proposed framework helps system operators to identify the key devices and consumers with high carbon emissions in UMESs, which can guide the formulation of effective carbon reduction strategies.

Author Contributions: Conceptualization, X.Z.; methodology, X.Z.; software, X.Z.; validation, X.Z., M.S., and M.B.; formal analysis, X.Z.; investigation, X.Z.; resources, X.Z.; data curation, X.Z.; writing—original draft preparation, X.Z.; writing—review and editing, X.Z., M.S., M.B., and Y.D.; visualization, X.Z.; supervision, Y.D.; project administration, Y.D.; funding acquisition, Y.D. All authors have read and agreed to the published version of the manuscript.

Funding: This research was supported by Science and Technology Projects of Guizhou Province ([2021]409).

Institutional Review Board Statement: Not applicable.

Informed Consent Statement: Not applicable.

Conflicts of Interest: The authors declare no conflict of interest.

Appendix A

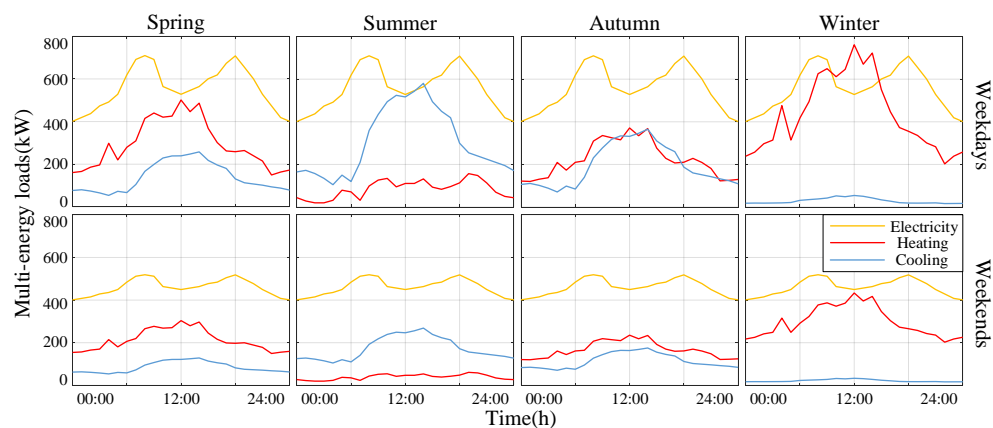


Figure A1. The electricity, heating and cooling loads for the EH in four seasons.

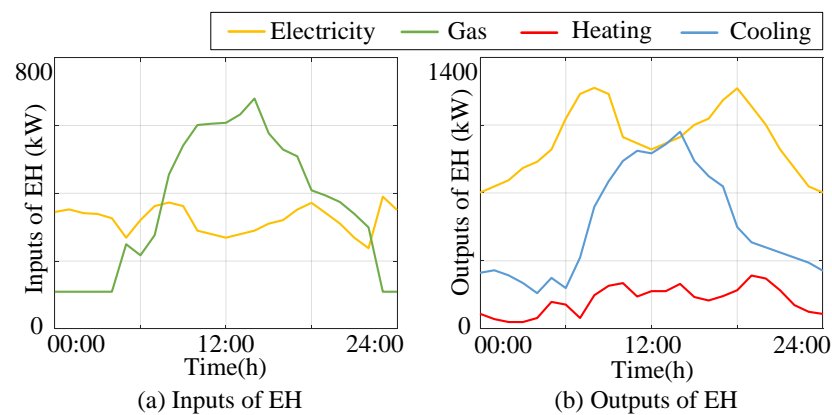


Figure A2. The inputs and outputs of EH on summer weekdays.

References

1. Olabi, A.; Obaideen, K.; Elsaid, K.; Wilberforce, T.; Sayed, E.T.; Maghrabie, H.M.; Abdelkareem, M.A. Assessment of the pre-combustion carbon capture contribution into sustainable development goals SDGs using novel indicators. *Renew. Sustain. Energy Rev.* **2021**, *153*, 111710. [CrossRef]
2. Accelerating the Transition from Coal to Clean Power. Available online: <https://ukcop26.org/energy/> (accessed on 17 March 2022).
3. Yang, X.; Shang, G.; Deng, X. Estimation, decomposition and reduction potential calculation of carbon emissions from urban construction land: Evidence from 30 provinces in China during 2000—2018. *Environ. Dev. Sustain.* **2021**, 1–18. [CrossRef]
4. Klüppel, H.-J. The Revision of ISO Standards 14040-3—ISO 14040: Environmental management—Life cycle assessment—Principles and framework—ISO 14044: Environmental management—Life cycle assessment—Requirements and guidelines. *Int. J. Life Cycle Assess.* **2005**, *10*, 165. [CrossRef]
5. Chau, C.-K.; Leung, T.M.; Ng, W.Y. A review on Life Cycle Assessment, Life Cycle Energy Assessment and Life Cycle Carbon Emissions Assessment on buildings. *Appl. Energy* **2015**, *143*, 395–413. [CrossRef]
6. Cheng, Y.; Zhang, N.; Wang, Y.; Yang, J.; Kang, C.; Xia, Q. Modeling Carbon Emission Flow in Multiple Energy Systems. *IEEE Trans. Smart Grid* **2019**, *10*, 3562–3574. [CrossRef]
7. Moser, A.; Muschick, D.; Gölles, M.; Nageler, P.; Schranzhofer, H.; Mach, T.; Tugores, C.R.; Leusbrock, I.; Stark, S.; Lackner, F.; et al. A MILP-based modular energy management system for urban multi-energy systems: Performance and sensitivity analysis. *Appl. Energy* **2019**, *261*, 114342. [CrossRef]
8. Gil, H.A.; Joos, G. Generalized Estimation of Average Displaced Emissions by Wind Generation. *IEEE Trans. Power Syst.* **2007**, *22*, 1035–1043. [CrossRef]
9. Chicco, G.; Mancarella, P. Assessment of the greenhouse gas emissions from cogeneration and trigeneration systems. Part I: Models and indicators. *Energy* **2008**, *33*, 410–417. [CrossRef]
10. Kang, C.; Zhou, T.; Chen, Q.; Xu, Q.; Xia, Q.; Ji, Z. Carbon Emission Flow in Networks. *Sci. Rep.* **2012**, *2*, 479. [CrossRef]
11. Kang, C.; Zhou, T.; Chen, Q.; Wang, J.; Sun, Y.; Xia, Q.; Yan, H. Carbon Emission Flow from Generation to Demand: A Network-Based Model. *IEEE Trans. Smart Grid* **2015**, *6*, 2386–2394. [CrossRef]
12. Wang, Y.; Qiu, J.; Tao, Y. Optimal Power Scheduling Using Data-Driven Carbon Emission Flow Modelling for Carbon Intensity Control. *IEEE Trans. Power Syst.* **2021**, 1–11. [CrossRef]
13. Zhang, X.; Chen, Y.; Yu, T.; Yang, B.; Qu, K.; Mao, S. Equilibrium-inspired multiagent optimizer with extreme transfer learning for decentralized optimal carbon-energy combined-flow of large-scale power systems. *Appl. Energy* **2017**, *189*, 157–176. [CrossRef]
14. Wang, Y.; Qiu, J.; Tao, Y.; Zhang, X.; Wang, G. Low-carbon oriented optimal energy dispatch in coupled natural gas and electricity systems. *Appl. Energy* **2020**, *280*, 115948. [CrossRef]
15. Zhao, H.; Li, B.; Lu, H.; Wang, X.; Li, H.; Guo, S.; Xue, W.; Wang, Y. Economy-environment-energy performance evaluation of CCHP microgrid system: A hybrid multi-criteria decision-making method. *Energy* **2021**, *240*, 122830. [CrossRef]
16. Bahlawan, H.; Poganietz, W.-R.; Spina, P.R.; Venturini, M. Cradle-to-gate life cycle assessment of energy systems for residential applications by accounting for scaling effects. *Appl. Therm. Eng.* **2020**, *171*, 115062. [CrossRef]
17. Khan, U.; Zevenhoven, R.; Tveit, T.-M. Evaluation of the Environmental Sustainability of a Stirling Cycle-Based Heat Pump Using LCA. *Energies* **2020**, *13*, 4469. [CrossRef]
18. Bian, B.; Du, Z.; Zhou, K.; Huang, T.; Lv, F. Optimal Planning Method of Integrated Energy System Considering Carbon Cost from the Perspective of the Whole Life Cycle. *IOP Conf. Ser. Earth Environ. Sci.* **2021**, *897*, 012021. [CrossRef]
19. Gautam, M.; Pandey, B.; Agrawal, M. Carbon Footprint of Aluminum Production: Emissions and Mitigation. In *Environmental Carbon Footprints*; Muthu, S.S., Ed.; Butterworth-Heinemann: Oxford, UK, 2018; Chapter 8; pp. 197–228.
20. Ye, S.; Ruan, W.; Wang, S.; Zhang, C. A bi-Level equivalent model of scheduling an energy hub to provide operating reserve for power systems. In Proceedings of the 2020 Tsinghua—HUST-IET Electrical Engineering Academic Forum, Beijing, China, 10–11 May 2020; pp. 1–7.

21. Kelly, K.; McManus, M.; Hammond, G. An energy and carbon life cycle assessment of industrial CHP (combined heat and power) in the context of a low carbon UK. *Energy* **2014**, *77*, 812–821. [[CrossRef](#)]
22. Moghaddam, I.G.; Saniei, M.; Mashhour, E. A comprehensive model for self-scheduling an energy hub to supply cooling, heating and electrical demands of a building. *Energy* **2016**, *94*, 157–170. [[CrossRef](#)]
23. Vaghefi, A.; Jafari, M.; Bisse, E.; Lu, Y.; Brouwer, J. Modeling and forecasting of cooling and electricity load demand. *Appl. Energy* **2014**, *136*, 186–196. [[CrossRef](#)]
24. China Electric Power Yearbook Committee. *China Electric Power Yearbook*; China Electric Power Press: Beijing, China, 2020.
25. Mancarella, P.; Chicco, G. Real-Time Demand Response from Energy Shifting in Distributed Multi-Generation. *IEEE Trans. Smart Grid* **2013**, *4*, 1928–1938. [[CrossRef](#)]